

Validating osteological correlates for the hepatic piston in the American Alligator (*Alligator mississippiensis*)

Clinton A Grand Pré^{Corresp., 1}, William Thielicke², Raul E Diaz Jr³, Brandon P Hedrick⁴, Ruth M Elsey^{5, 6}, Emma R Schachner^{Corresp. 7}

¹ Cell Biology and Anatomy, Louisiana State University Health Sciences Center, New Orleans, LA, USA

² OPTOLUTION Messtechnik GmbH, Loerrach, Germany

³ Department of Biological Sciences, California State University Los Angeles, Los Angeles, CA, USA

⁴ Department of Biomedical Sciences, Cornell University, Ithaca, NY, United States

⁵ Louisiana Department of Wildlife and Fisheries, Grand Chenier, LA, USA

⁶ Unaffiliated, 728 Saratoga Drive, Tennessee, USA

⁷ Department of Physiological Sciences / College of Veterinary Medicine, University of Florida, Gainesville, Florida, USA

Corresponding Authors: Clinton A Grand Pré, Emma R Schachner

Email address: cgran9@lsuhsc.edu, eschachner@ufl.edu

Unlike the majority of sauropsids, which breathe primarily through costal and abdominal muscle contractions, extant crocodylians have evolved the hepatic piston pump, a unique additional ventilatory mechanism powered by the diaphragmaticus muscle. This muscle originates from the bony pelvis, wrapping around the abdominal viscera, extending cranially to the liver. The liver then attaches to the caudal margin of the lungs, resulting in a sub-fusiform morphology for the entire “pulmo-hepatic-diaphragmatic” structure. When the diaphragmaticus muscle contracts during inspiration, the liver is pulled caudally, lowering pressure in the thoracolumbar cavity, and inflating the lungs. It has been established that the hepatic piston pump requires the liver to be displaced to ventilate the lungs, but it has not been determined if the lungs are freely mobile or if the pleural tissues stretch ventrally. It has been hypothesized that the lungs are able to slide craniocaudally with the liver due to the smooth internal ceiling of the thoracolumbar cavity. We assess this through ultrasound video and demonstrate quantitatively and qualitatively that the pulmonary tissues are sliding craniocaudally across the interior thoracolumbar ceiling in actively ventilating live juvenile, sub-adult, and adult individuals ($n = 7$) of the American alligator (*Alligator mississippiensis*) during both natural and induced ventilation. The hepatic piston is a novel ventilatory mechanism with a relatively unknown evolutionary history. Questions related to when and under what conditions the hepatic piston first evolved have previously been left unanswered due to a lack fossilized evidence for its presence or absence. By functionally correlating specific characters in the axial skeleton to the hepatic piston, these osteological correlates can be applied to fossil taxa to reconstruct

the evolution of the hepatic piston in extinct crocodylomorph archosaurs.

**Validating osteological correlates for the hepatic piston in the American Alligator
(Alligator mississippiensis)**

3 Clinton Andrew Grand Pré¹, William Thielicke², Raul E. Diaz Jr³, Brandon P. Hedrick⁴, Ruth
4 M. Elsey^{5,6}, Emma R. Schachner⁷

5

6 ¹ Department of Cell Biology and Anatomy, School of Medicine, Louisiana State University
7 Health Sciences Center, New Orleans, LA, USA

8 ² OPTOLUTION Messtechnik GmbH, Loerrach, Germany

9 ³ Department of Biological Sciences, California State University Los Angeles, Los Angeles, CA,
10 USA

11 ⁴ Department of Biomedical Sciences, College of Veterinary Medicine, Cornell University,
12 Ithaca, NY, USA

13 ⁵ Louisiana Department of Wildlife and Fisheries, 5476 Grand Chenier Highway, Grand Chenier,
14 Louisiana, USA

15 ⁶ 728 Saratoga Drive, Murfreesboro, Tennessee, USA

16 ⁷ Department of Physiological Sciences, College of Veterinary Medicine, University of Florida,
17 Gainesville, FL, USA

18

19 Corresponding Author:

20 Clinton Andrew Grand Pré¹

21 1901 Perdido Street, New Orleans, LA, 70112, USA

22 Email Address: cgran9@lsuhsc.edu

23

24

25

Abstract

27 Unlike the majority of sauropsids, which breathe primarily through costal and abdominal
28 muscle contractions, extant crocodylians have evolved the hepatic piston pump, a unique
29 additional ventilatory mechanism powered by the diaphragmaticus muscle. This muscle
30 originates from the bony pelvis, wrapping around the abdominal viscera, extending cranially to
31 the liver. The liver then attaches to the caudal margin of the lungs, resulting in a sub-fusiform
32 morphology for the entire “pulmo-hepatic-diaphragmatic” structure. When the diaphragmaticus
33 muscle contracts during inspiration, the liver is pulled caudally, lowering pressure in the
34 thoracolumbar cavity, and inflating the lungs. It has been established that the hepatic piston
35 pump requires the liver to be displaced to ventilate the lungs, but it has not been determined if
36 the lungs are freely mobile or if the pleural tissues stretch ventrally. It has been hypothesized that
37 the lungs are able to slide craniocaudally with the liver due to the smooth internal ceiling of the
38 thoracolumbar cavity. We assess this through ultrasound video and demonstrate quantitatively
39 and qualitatively that the pulmonary tissues are sliding craniocaudally across the interior
40 thoracolumbar ceiling in actively ventilating live juvenile, sub-adult, and adult individuals (n =
41 7) of the American alligator (*Alligator mississippiensis*) during both natural and induced
42 ventilation. The hepatic piston is a novel ventilatory mechanism with a relatively unknown
43 evolutionary history. Questions related to when and under what conditions the hepatic piston first
44 evolved have previously been left unanswered due to a lack fossilized evidence for its presence
45 or absence. By functionally correlating specific characters in the axial skeleton to the hepatic
46 piston, these osteological correlates can be applied to fossil taxa to reconstruct the evolution of
47 the hepatic piston in extinct crocodylomorph archosaurs.

Introduction

49 Non-avian sauropsids primarily utilize their costal and abdominal musculature to power
50 their breath cycles (Brainerd and Owerkowicz, 2006). Crocodylians developed an additional
51 method for ventilation utilizing the novel diaphragmaticus muscle termed the hepatic piston
52 pump (Boelaert, 1942; Carrier and Farmer, 2000; Claessens, 2004; Claessens, 2009; Uriona and
53 Farmer, 2008). The diaphragmaticus muscle originates from the pelvis, attaches to the pubic
54 apron and gastralia ventrally, and travels cranially, inserting along the liver capsule and
55 pericardium (Fig. 1A, B). When the diaphragmaticus muscle contracts, it pulls the liver and
56 viscera caudally, serving to generate negative pressure in the lungs and the cranial part of the
57 thoracolumbar cavity, inducing inspiration (Claessens, 2009; Farmer and Carrier, 2000b; Gans
58 and Clark, 1976). Exhalation primarily occurs via passive relaxation of the diaphragmaticus
59 and/or active contraction of the rectus abdominis muscle and costal musculature resulting in the
60 liver and all viscera sliding cranially (Claessens, 2009; Farmer and Carrier, 2000b; Gans and
61 Clark, 1976; Uriona and Farmer, 2008).

62 The diaphragmaticus muscle is not homologous to the mammalian diaphragm. The
63 mammalian diaphragm is innervated by the phrenic nerves of the cervical plexus and the
64 diaphragmaticus is innervated by spinal nerves 22 and 23. Further, the rectus abdominis and
65 diaphragmaticus muscles are used synchronously for diving, and most likely evolved from the
66 same abdominal muscle group primarily for use in aquatic environments to control pitch and roll
67 during diving in *A. mississippiensis* by shifting the center of mass (Carrier and Farmer, 2000;
68 Uriona and Farmer, 2006). The evolutionary origin of the hepatic piston has been hypothesized
69 to have been associated with the secondary aquatic habitat of crocodylians, placing the evolution
70 of the diaphragmaticus muscle after the split between Pseudosuchia and Avemetatarsalia, making

71 it distinct from the respiratory anatomy found in non-avian dinosaurs and birds (Claessens and
72 Vickaryous, 2012; Uriona and Farmer, 2008).

73 Evaluating the occurrence of soft tissue structures in the fossil record is difficult and best
74 done using osteological correlates; bony anatomical structures or features that can be
75 morphologically linked to soft tissue in extant taxa (Lauder, 1995; Witmer, 1995). The shift from
76 a terrestrial to a semi-aquatic or aquatic niche in extinct and extant crocodylians is associated
77 with a series of correlates related to cranium shape, body size, or derived from the hindlimb and
78 pelvis as they relate to locomotion (Benson and Butler, 2011; Chamero et al., 2013; Hedrick et
79 al., 2022; Hua, 2003; Iijima et al., 2018; Iijima and Kubo, 2019; Mannion et al., 2015; Molnar et
80 al., 2015; Nesbitt, 2011; Parrish, 1986; Parrish, 1987; Salisbury and Frey, 2000; Salisbury et al.,
81 2006; Stockdale and Benton, 2021; Sullivan, 2015; Wilberg, 2015; Wilberg et al., 2019; Young
82 et al., 2012a; Young et al., 2012b). For example, elongate limbs, dorsoventrally tall crania, and
83 well-developed fourth trochanters of femora are associated with terrestrial habitats while paddle-
84 like limbs and a hypocercal tail fin are associated with fully marine environments (Wilberg,
85 2015; Wilberg et al., 2019; Young et al., 2012a; Young et al., 2012b).

86 The smooth interior ceiling of the thoracolumbar cavity in *A. mississippiensis* is
87 associated with the following distinct osteological characteristics (Fig. 2): (1) the parapophysis
88 migrates from the vertebral centrum to the transverse process at or after thoracic vertebra three
89 (T3), and progressively out along the transverse process towards the diapophysis sequentially;
90 (2) the presence of broad flat and progressively elongate transverse processes; (3) a lack of
91 forked ribs beyond T3 that create a distinctly smooth dorsal ceiling; and, (4) a rib-free lumbar
92 region. We propose that these features defining a smooth thoracolumbar ceiling (Fig. 3) allow
93 the lungs, liver, and viscera to slide unimpeded, and are therefore osteological correlates for the

94 hepatic piston pump. Since the diaphragmaticus muscle has been proposed to be primarily a
95 muscle that evolved for an aquatic environment (Uriona and Farmer, 2006), these osteological
96 correlates may be useful in identifying when the hepatic piston first evolved and if this
97 evolutionary event coincided with when the ancestors of extant crocodylians moved into semi-
98 aquatic and/or aquatic habitats (Brocklehurst et al., 2018; Schachner et al., 2009; Schachner et
99 al., 2011). Despite this hypothesis, these correlates have yet to be functionally validated in extant
100 crocodylians. Here, using ultrasound data for seven individuals of *A. mississippiensis* across a
101 growth series (juvenile to adult), we qualitatively and quantitatively demonstrate a functional
102 relationship between a smooth interior thoracolumbar ceiling and the hepatic piston and
103 recommend a distinct set of morphological characters as osteological correlates that can be used
104 to reconstruct the evolutionary history of the hepatic piston in the fossil record.

Materials and Methods

Anatomical modeling and Microcomputed Tomography (μ CT)

107 To illustrate the diaphragmaticus muscle, a μ CT scan of one sub-adult 3.4 kg *A.*
108 *mississippiensis* (identified as Hamilcar Barca for this project) was obtained from a privately
109 owned facility (Scales and Tales Utah) for clinical purposes (unrelated to this study) and donated
110 for this project. The entire alligator was scanned in a prone position, during a natural apnea, at a
111 resolution of 2 mm slices (80 kVp, 60 mA). The skeleton and lungs of this individual were
112 segmented into a surface model using Avizo 7.1 (Thermo Fisher Scientific) and followed the
113 methods of Lawson et al. (2021) and Schachner et al. (2023). The diaphragmaticus muscle and
114 liver were then illustrated into model using Adobe Photoshop (Fig. 1A, B).

115 *Ultrasound Data Collection*

116 A total of 170 individual 16-second ultrasound videos were collected from three juvenile,
117 two sub-adult, and two adult *A. mississippiensis* ($n = 7$) (see Table 1 for the names and snout-
118 vent lengths [SVL] of the specimens). Individuals were scanned at Louisiana State University
119 Health Sciences Center (LSUHSC) in New Orleans and at the Rockefeller Wildlife Refuge in
120 Grand Chenier, Louisiana. Two individuals were part of the collection of Dr. Raul Diaz (then
121 Southeastern Louisiana University) and five individuals were collected by Dr. Ruth Elsey and
122 staff (Rockefeller Wildlife Refuge). All research conducted on living individuals was approved
123 by the LSUHSC Institutional Animal Care and Use Committee (IACUC #6341).

124 The animals were not sedated and were scanned in an at-rest, prone, stationary position.
125 While at rest, alligators can enter prolonged periods of apnea. Recordings were taken both during
126 natural breathing, when the individual was compliant and breathed deeply on its own, and during
127 induced breathing. Induced breathing was achieved by giving individuals a 5% CO₂, balance N₂
128 gas following the procedures outlined in Douse and Mitchell (1992) and Uriona and Farmer
129 (2006). Induced breathing reduced the duration of the apneas and allowed for more breaths to be
130 recorded within the video duration. A recording time of 16 seconds was selected to allow
131 adequate time for the animal to take several breaths. Gas was pumped through a polyethylene
132 tube to a bag that was fitted over the nares and mouth of each alligator. Individuals did not
133 breathe the 5% CO₂, balance N₂ for longer than three minutes at a time. All measurements were
134 taken with an ultrasound machine using a 12-L probe and penetration depths ranged from two
135 cm for the juveniles to seven cm for the adults. The measurements were collected at four
136 locations (axillary, mid-thoracic, hepatic, and post-hepatic) on the left lateral side of the animal
137 in the coronal plane using consistent anatomical landmarks (Fig.1C). Individual animals were

138 named for ancient military figures from Carthage, the Roman Republic, and one fictional British
139 MI6 agent for identification.

140 *Ultrasound Measures*

141 Displacement was quantified first by visually establishing the most cranial and most
142 caudal positions of the pleural-hepatic margin during the breath cycle in each video. Frames
143 corresponding with the extremes of the breath cycle were then exported into Adobe Illustrator
144 (Adobe Inc., 2019) and superimposed. The distance between the most cranial and most caudal
145 positions of the cranial hepatic margin was measured by drawing a line segment between them,
146 the length of which was recorded and scaled to the image size using the scale bars in the
147 ultrasound videos. To ensure consistency, this process was repeated three times and averaged for
148 each video. Results were reported both as total length in centimeters and as a percentage of SVL.
149 This technique, while accurate, could be used only at the hepatic margin position where clear
150 anatomical landmarks could be identified visually.

151

152 *PIVlab*

153 To assess movement at other locations where visual assessment and direct measurement
154 were not possible, we utilized a modified version of PIVlab (Thielicke and Sonntag, 2021), an
155 open-source program for digital particle image velocimetry (DPIV). DPIV is an analysis
156 technique that can be used to map the spatially resolved velocity or displacement of particle
157 images. DPIV is increasingly used in research areas other than fluid dynamics such as measuring
158 the displacement of diverse textures in digital image data (Thielicke and Sonntag, 2021). In the
159 modified version of PIVlab, one or multiple user-generated region of interest (ROI) rectangles
160 were created of any size in any position on the video. Once the ROI was selected, pre-processing

161 image enhancements, Contrast Limited Adaptive Histogram Equalization–CLAHE (Pizer et al.,
162 1987) and background subtraction (Thielicke and Sonntag, 2021), were performed to increase the
163 signal-to-noise ratio. Cross-correlation was performed in the spatial domain (direct cross-
164 correlation), and as repeated correlation, where the correlation matrices of slightly shifted
165 evaluation windows were multiplied to maximize the signal-to-noise ratio. The displacement of
166 the ROI was determined frame by frame and the displacement was used to offset the ROI in the
167 following frame, enabling the user to lock on the selected pixel pattern in the ultrasound images
168 over time.

169 Of 170 videos recorded, we were able to measure displacement in 53 videos using
170 PIVlab. The remaining videos could not be processed due to issues with the ultrasound (e.g.,
171 dark shadows deep to bone that interfered with the program’s ability to track movement) or due
172 to animal movement. It was also evident that tracking boxes frequently lagged behind the tissue
173 in the target window in successful videos, sometimes dramatically. Although these videos
174 demonstrated tissue movement, they underestimated the amount of movement.

Results

176 Ultrasound data (see supplementary materials for ultrasound videos) demonstrate the
177 craniocaudal transition of the pulmonary pleura and liver during breathing relative to the
178 vertebrae at all four measured positions (axillary, mid-thoracic, hepatic, and post-hepatic) in all
179 seven individuals (examples of each location are available in Supplemental Information (SI)
180 Video S1-S8. The amount the pulmonary pleura displacement differs at the four positions of
181 measurement. In the axillary position (just caudal and slightly dorsal to the forelimb) the
182 pulmonary pleura can be observed sliding just deep to the vertebrae and ribs in small amounts
183 (Video S1). In the mid-thoracic position (halfway between the pleura/hepatic margin and the
184 axilla), the pulmonary pleura can be observed sliding deep to the thoracic vertebrae and

185 displacing slightly more than in the axillary position. There are no clear anatomical landmarks
186 that distinguish relative positions of pleura at these locations, so only qualitative observations
187 about the distance of displacement can be made, but the ultrasound videos demonstrate that
188 displacement increases moving caudally (Videos S1-S8). At the hepatic position the pleura is
189 visualized attaching to the cranial aspect of the liver and the diaphragmaticus muscle is attaching
190 to the caudal aspect of the liver. At this position the ultrasound data demonstrate that the
191 displacement is larger than at the mid-thoracic or axillary positions (Videos S4-S7). At the
192 hepatic margin during inhalation, contraction of the diaphragmaticus is visualized, which causes
193 the liver and lung pleura to be pulled caudally. During exhalation, the diaphragmaticus relaxes
194 and the liver and the pleura move cranially in tandem (Video S4-S7). At the post-hepatic position
195 the diaphragmaticus and the GI can be visualized moving with the liver and the lung pleura
196 (Video S8). At the hepatic margin, the entire contents of the pleuroperitoneal cavity are
197 visualized moving together (Videos S1-S8).

198 The translation of the viscera is tracked via PIVlab at the hepatic position where the lung
199 pleura attaches to the cranial aspect of the liver because the liver is a clear anatomical landmark
200 that interfaces directly with the lung pleura. (Fig. 4). Direct measures of displacement are
201 measured at the hepatic margin position for every animal (Table 2). The relationship between the
202 amount of displacement and the use of 5% CO₂, balance N₂ is not significant suggesting that
203 induced breaths and natural breaths are similar in displacement (Fig. 5A). The amount of
204 displacement varies both between breaths in each individual and between individuals. Average
205 displacements for each individual ranges between 2.90% SVL in Claudius and 8.39% SVL in
206 Hannibal (Table 2). The greatest displacements relative to SVL are measured in the smallest
207 individuals (15.78% of the SVL in Hannibal, 11.11% in Bond). The smallest displacements

208 relative to SVL are in mid-sized to large alligators (Scipio, 1.07 %, SVL 31 cm; Claudius,
209 1.46%, SVL 56 cm; Archimedes, 1.54%, SVL 89 cm). The relationship between the amount of
210 displacement and SVL is not significant and does not scale with size (Fig. 5B).

211

Discussion

213 *Measuring Displacement*

214 The main aim of this work was to evaluate if the lung pleura was moving across the
215 smooth interior ceiling of the thoracolumbar cavity during ventilation with the hepatic piston,
216 and if so, to establish associated osteological correlates for this ventilatory mechanism in *A.*
217 *mississippiensis*. The lung pleura sliding against the smooth ceiling of the thoracolumbar cavity
218 was evident in all videos where deep breaths occurred, with maximum liver displacement
219 ranging from 4.24% to 15.78% SVL. It is likely this study does not capture maximum inspiratory
220 capacity nor the full range of displacement possible under varying physiological conditions. *A.*
221 *mississippiensis* likely breathes more deeply during or after exercise or while diving (Farmer and
222 Carrier, 2000a; Munns et al., 2005; Uriona and Farmer, 2006; Uriona and Farmer, 2008).
223 Additionally, four of seven individuals were wild caught and thus were not fasted before
224 analysis: Eating a large meal (>15% of body mass) can decrease the animal's vital capacity by up
225 to 25% (Uriona and Farmer, 2006), which would potentially decrease the maximum
226 displacement measured in these wild individuals. However, it is unlikely these wild-caught
227 individuals ate a large meal at the time of capture, they were caught during the fall season when
228 feeding frequency decreases substantially (Lance, 2003). Other external physiological variables
229 that may have an effect on inspiratory capacity include ambient temperature (Munns et al.,

230 2012), if the animal is on land or in water (Gans and Clark, 1976; Uriona and Farmer, 2006), and
231 if the animal is standing (Uriona and Farmer, 2006).

232 There are also many other internal physiological variables that can lead to substantial
233 changes in total displacement via the hepatic piston. Crocodylians can switch between
234 costal/abdominal dominant or hepatic dominant ventilation, greatly varying the amount the
235 hepatic piston contributes to inspiration (Brainerd and Owerkowicz, 2006; Brocklehurst et al.,
236 2017; Claessens, 2009; Farmer and Carrier, 2000b; Gans and Clark, 1976; Munns et al., 2012).
237 Further, crocodylians can enter long periods of apnea (Gans and Clark, 1976; Uriona and Farmer,
238 2006), and can increase their total tidal volume (rather than breathing frequency) during periods
239 of hypercapnia (Claessens, 2009; Wang and Warburton, 1995). Due to the propensity for apnea,
240 we used 5% CO₂, balance N₂ gas to induce deep breaths (Douse and Mitchell, 1992; Uriona and
241 Farmer, 2006) but did not find a statistical relationship between the amount of displacement and
242 the use of 5% CO₂, balance N₂ gas (Fig. 5A). If breathing the 5% CO₂, balance N₂ gas was
243 putting the individuals in a state of hypoxia we would expect to see an increase in displacement
244 when the individuals breathed the 5% CO₂, balance N₂ gas. Instead, we observed no measurable
245 difference when animals breathed the gas or did not. Nevertheless, the ability for crocodylians to
246 change the dominant muscles of inspiration and change the frequency and intensity of apnea
247 suggests that the displacement measured does not represent the displacement possible under
248 various internal conditions.

249 Crocodylians can also change the tension of the abdominal wall and gastralia (Farmer and
250 Carrier, 2000b; Gans and Clark, 1976), have a rotating pubis that changes the potential caudal
251 extent of visceral displacement (Claessens, 2004; Claessens, 2009; Farmer and Carrier, 2000b),
252 and can maintain or change the pressure gradient on either side of the post-pulmonary septum

253 (PPS) (Cramberg et al., 2022). Klein and Owerkowicz (2006) discuss that the “diaphragmaticus-
254 endowed PPS” can assist with cranial visceral displacement to avoid lung collapse. It should be
255 noted that Klein and Owerkowicz (2006) often reference the crocodilian diaphragmaticus and
256 PPS functionally together, but they are distinct anatomical structures (Cramberg et al., 2022).
257 Despite the known ability of crocodilians to drastically change how much the hepatic piston
258 contributes to inspiration, our measures of displacement are consistent with observations from
259 Schachner et al. (2022) and Claessens (2009).

260 μ CT is a useful method for evaluating the potential of lung movement and of inspiratory
261 capacity in crocodilians. Schachner et al. (2022) imaged multiple specimens of live and deceased
262 Cuvier’s dwarf caiman (*Paleosuchus palpebrosus*) in different states: post-prandial, fasting, open
263 to atmosphere, and at total lung capacity. Post-prandial individuals had cranially displaced lungs
264 up to five vertebral segments compared to a fasted state. Individuals of deceased hatchling *P.*
265 *palpebrosus* that had fully inflated lungs had a cranial displacement of 1.5 vertebral lengths
266 relative to individuals scanned that were open to atmosphere. This demonstrates the large
267 variability in crocodilian lung volume and position and is consistent with the results found here
268 for *A. mississippiensis*. In the ultrasound videos at the pleural hepatic margin the pleura and liver
269 are routinely sliding across one to three vertebral lengths (see supplementary materials on Data
270 Dryad for all ultrasound videos). This is also consistent with Claessens (2009), who reports,
271 using cineradiographic techniques, an average displacement of the cranial surface of the liver of
272 1.4 vertebral segment in juvenile individuals of *A. mississippiensis*.

273 We did not find a correlation between size and displacement (Fig. 5B). Gans and Clark
274 (1976) report, using EMG data in *C. crocodilus*, that breath frequency decreases in larger
275 animals. This study includes 20 individuals that range in size from 400 g to 7.5 kg. Claessens

276 (2009) in a cineradiographic study of five juvenile *A. mississippiensis*, ranging from 55–115 cm
277 total length, reported liver displacement is larger in larger individuals. Munns et al. (2012)
278 reported personal observations that the diaphragmaticus muscle in juvenile crocodylians are thin
279 and translucent and thicker and more well-developed in adults. We confirm this observation
280 (pers. obs., CGP and ERS) in dissections of *A. mississippiensis*. The limitations of correlating
281 size and displacement include that Claessens (2009) and Gans and Clark (1976) studies contain
282 no adults. Further, all studies, including this one, are limited in that crocodylians are known to
283 vary their reliance on the hepatic piston during ventilation, therefore capturing the total variation
284 is difficult for any one study. This is not a physiologic study on all possible variation in the
285 displacement via the hepatic piston. To vigorously study the relationship between size and
286 hepatic piston use we suggest a mixed methodology that includes XROMM and
287 electromyography on many individuals ranging in size from hatchling to adults in numerous
288 physiologic conditions.

289

290 ***PIVLAB***

291 PIVlab was useful in providing clear respiration curves (Fig. 4). Our measurements of
292 displacement in PIVlab underestimated displacement compared to the manual measurements at
293 the hepatic margin. This is not the result of an inherent flaw with PIVlab but is related to the
294 nature of ultrasound data. Ultrasound data from the thoracic region commonly have shadows
295 from ribs that interrupt tracking in PIVlab and have lower contrast between the target and
296 background ultrasound scatter. The human eye and manual tracking can follow movement that
297 an automated program cannot. Also, PIVlab functions by maintaining the tracking box in every
298 frame of the video. A shadow that may darken halfway through the video is enough for PIVlab to

299 lose its target: The PIVlab algorithm tracks the most statistically significant pixel pattern. If a
300 shadow dominates the tracked region, then the algorithm will tend to track the shadow. The
301 manual procedure needs a clear frame of only the most cranial and most caudal aspects of the
302 breath to measure the displacement. However, this initial work and prior studies that have used
303 DPIV with ultrasound (Farron et al., 2009; Korstanje et al., 2009; Korstanje et al., 2010;
304 Korstanje et al., 2012; Loram et al., 2006) demonstrate that there is promise in advancing PIVlab
305 technology to work more consistently with ultrasound data.

306 *Heterogeneity of lung movements*

307 When describing the lung of the Nile crocodile (*Crocodylus niloticus*), Perry (1988)
308 states that it will “tend to fuse with the parietal pleural surface” and therefore the lung tissue
309 stretches instead of sliding during inspiration via the hepatic piston (particularly the cranial half).
310 There are two main points in Perry’s (1988) work that are of interest: (1) the *C. niloticus* lung is
311 more strongly attached to the parietal pleura cranially than caudally, and as a consequence, (2) in
312 the caudal half of the lung, the pleural tissue is stretching instead of sliding. It is possible that the
313 specimens evaluated by Perry with fusion between the visceral and parietal pleura were
314 pathologic, but this needs to be investigated further in other adult specimens of *C. niloticus*. We
315 qualitatively demonstrate in this study that the amount of pleural displacement increases moving
316 from cranially to caudally in all individuals via the ultrasound videos in *A. mississippiensis*.
317 There is minimal displacement in the axillary position, where the ribs are forked, but the visceral
318 pleural tissues do not appear to be fused with the parietal pleural. The largest amount of pleural
319 displacement is in the hepatic position where the thoracic vertebrae are wide and the ribs are flat,
320 creating a smooth surface (on the interior thoracic ceiling) on which the lung tissue can either
321 expand or slide freely. However, studies on the potential heterogeneous mechanical properties of

322 the lung pleura may reveal more information related to the structural changes in the lung tissue
323 that Schachner et al. (2022) and Perry (1988) observed and how this varies across Crocodylia.
324 Schachner et al (2013) did not find any fusion between the visceral and parietal pleural described
325 for *C. niloticus* by Perry (1988) and there may be intraspecific variation or pathologies
326 associated with fusion observed in some of these animals. It is possible that adhesions occur
327 variably and impact hepatic piston function. Additional investigation into differential movements
328 of the alligator pulmonary tissues will also reveal if there are any functional relationships
329 between differential regional mobility/immobility of the pulmonary pleura and the architecture
330 of the bronchial tree.

331

332 ***Evolution of the Hepatic Piston***

333 Of all the various morphologically and ecologically diverse pseudosuchian groups that
334 thrived during the Late Triassic period, only small, terrestrial crocodylomorph pseudosuchians
335 survived the Triassic/Jurassic (Tr-J) mass extinction ~200 million years ago (Butler et al., 2011;
336 Nesbitt, 2011; Wilberg et al., 2019). These small gracile-limbed reptiles were the terrestrial
337 ancestor to all crown-group semi-aquatic extant crocodylians (Nesbitt, 2011). Following the Tr-J
338 extinction event, Crocodylomorpha quickly diversified and these animals were found in a wide
339 array of niches by the Middle Cretaceous, ranging from fully marine to terrestrial localities, and
340 potentially even arboreal habitats (Mannion et al., 2015; Wilberg et al., 2019). It has been
341 hypothesized that crocodylomorph archosaurs transitioned from terrestrial to semi-aquatic or to
342 marine environments multiple times (Lessner et al., 2023; Schwab et al., 2020; Wilberg et al.,
343 2019). Given the hypothesis that the hepatic piston evolved in association with diving by
344 controlling pitch and roll (Uriona and Farmer, 2008), establishing when the hepatic piston first

345 evolved may refine our understanding of the complex terrestrial and aquatic evolution of
346 crocodylomorphs. Our proposed osteological correlates for the hepatic piston offer a novel set of
347 postcranial characters that can be used to evaluate this environmental history.

348

Conclusions

350 Here we establish a functional relationship between previously described osteological
351 correlates in the axial skeleton of the American alligator with the ventilatory movements of the
352 hepatic piston mechanism. The loss of the forked ribs cranially, combined with the broadening
353 and flattening of the transverse processes and a rib-free lumbar region, results in a smooth
354 interior ceiling of the thoracolumbar cavity, allowing the pleura to slide cranially/caudally during
355 ventilation. Visualization of the sliding pleura via ultrasound identifies the functional
356 relationship between axial skeletal morphology and pleural displacement, validating these
357 osteological correlates which can be utilized in reconstructing the origin and evolution of the
358 hepatic piston ventilatory mechanism in extinct crocodylomorph archosaurs.

Acknowledgments

360 We thank Dwayne LeJeune, Mickey Miller, and Nick Latiolais for assistance with
361 capture and handling of alligators used in the study. CG Farmer and Dan Malleske were integral
362 to the primary exploratory phase of this work. Annette Gray and Adam Lawson provided critical
363 assistance with collecting the ultrasound data. Special thank you to Scales and Tails Utah for
364 permission to use a scan of one their animals, and Scott Echols DVM for providing imaging data.

365

References

367 **Benson, R. B. J. and Butler, R. J.** (2011). Uncovering the diversification history of
368 marine tetrapods: ecology influences the effect of geological sampling biases. *Geological*
369 *Society, London, Special Publications* **358**, 191-208.

- 370 **Boelaert, R.** (1942). Sur la physiologie de la respiration de l'Alligator mississippiensis.
371 *Archives Internationales de Physiologie* **52**, 57-72.
- 372 **Brainerd, E. L. and Owerkowicz, T.** (2006). Functional morphology and evolution of
373 aspiration breathing in tetrapods. *Respiratory Physiology & Neurobiology* **154**, 73-88.
- 374 **Brocklehurst, R. J., Moritz, S., Codd, J., Sellers, W. I. and Brainerd, E. L.** (2017).
375 Rib kinematics during lung ventilation in the American alligator (*Alligator mississippiensis*): an
376 XROMM analysis. *Journal of Experimental Biology* **220**, 3181-3190.
- 377 **Brocklehurst, R. J., Schachner, E. R. and Sellers, W. I.** (2018). Vertebral
378 morphometrics and lung structure in non-avian dinosaurs. *Royal Society Open Science* **5**,
379 10.1098/rsos.180983.
- 380 **Butler, R. J., Brusatte, S. L., Reich, M., Nesbitt, S. J., Schoch, R. R. and Hornung, J.**
381 **J.** (2011). The sail-backed reptile *Ctenosauriscus* from the latest Early Triassic of Germany and
382 the timing and biogeography of the early archosaur radiation. *PLoS ONE* **6**,
383 10.1371/journal.pone.0025693.
- 384 **Carrier, D. R. and Farmer, C. G.** (2000). The integration of ventilation and locomotion
385 in archosaurs. *American Zoologist* **40**, 87-100.
- 386 **Chamero, B., Buscalioni, Á. D. and Marugán-Lobón, J.** (2013). Pectoral girdle and
387 forelimb variation in extant Crocodylia: the coracoid–humerus pair as an evolutionary module.
388 *Biological Journal of the Linnean Society* **108**, 600-618.
- 389 **Claessens, L. P.** (2004). Archosaurian respiration and the pelvic girdle aspiration
390 breathing of crocodyliforms. *Proceedings of the Royal Society of London B: Biological Sciences*
391 **271**, 1461-1465.
- 392 **Claessens, L. P.** (2009). A cineradiographic study of lung ventilation in *Alligator*
393 *mississippiensis*. *Journal of Experimental Zoology Part A: Ecological Genetics and Physiology*
394 **311**, 563-585.
- 395 **Claessens, L. P. A. M. and Vickaryous, M. K.** (2012). The evolution, development, and
396 skeletal identity of the Crocodylian pelvis: Revisiting a forgotten scientific debate. *Journal of*
397 *Morphology* **273**, 1185-1198.
- 398 **Cramberg, M., Greer, S. and Young, B. A.** (2022). The functional morphology of the
399 postpulmonary septum of the American alligator (*Alligator mississippiensis*). *Anat Rec*
400 (*Hoboken*) **305**, 3055-3074.
- 401 **Douse, M. and Mitchell, G.** (1992). Effects of vagotomy on ventilatory responses to
402 CO₂ in alligators. *Respiration Physiology* **87**, 63-76.
- 403 **Farmer, C. G. and Carrier, D. R.** (2000a). Ventilation and gas exchange during
404 treadmill locomotion in the american alligator (*Alligator mississippiensis*). *The Journal of*
405 *Experimental Biology* **203**, 1671-1678.
- 406 **Farmer, C. G. and Carrier, D. R.** (2000b). Pelvic aspiration in the American alligator
407 (*Alligator mississippiensis*). *Journal of Experimental Biology* **203**, 1679-87.
- 408 **Farron, J., Varghese, T. and Thelen, D. G.** (2009). Measurement of tendon strain
409 during muscle twitch contractions using ultrasound elastography. *IEEE Transactions on*
410 *ultrasonics, ferroelectrics, and frequency control* **56**, 27-35.
- 411 **Gans, C. and Clark, B.** (1976). Studies on ventilation of *Caiman crocodilus* (Crocodylia:
412 Reptilia). *Respiration Physiology* **26**, 285-301.
- 413 **Hedrick, B. P., Schachner, E. R. and Dodson, P.** (2022). Alligator appendicular
414 architecture across an ontogenetic niche shift. *The Anatomical Record* **305**, 10.1002/ar.24717.

- 415 **Hua, S.** (2003). Locomotion in marine mesosuchians (Crocodylia): the contribution of
416 the locomotion profiles. *Neues Jahrbuch für Geologie und Paläontologie-Abhandlungen*, 139-
417 152.
- 418 **Iijima, M., Kubo, T. and Kobayashi, Y.** (2018). Comparative limb proportions reveal
419 differential locomotor morphofunctions of alligatoroids and crocodyloids. *R Soc Open Sci* **5**,
420 171774.
- 421 **Iijima, M. and Kubo, T.** (2019). Comparative morphology of presacral vertebrae in
422 extant crocodylians: taxonomic, functional and ecological implications. *Zoological Journal of*
423 *the Linnean Society* **186**, 1006-1025.
- 424 **Klein, W. and Owerkowicz, T.** (2006). Function of intracoelomic septa in lung
425 ventilation of amniotes: lessons from lizards. *Physiological and Biochemical Zoology* **79**, 1019-
426 1032.
- 427 **Korstanje, J.-W. H., Selles, R. W., Stam, H. J., Hovius, S. E. R. and Bosch, J. G.**
428 (2009). Dedicated ultrasound speckle tracking to study tendon displacement. In *Medical Imaging*
429 *2009: Ultrasonic Imaging and Signal Processing*.
- 430 **Korstanje, J. W., Selles, R. W., Stam, H. J., Hovius, S. E. and Bosch, J. G.** (2010).
431 Development and validation of ultrasound speckle tracking to quantify tendon displacement.
432 *Journal of Biomechanics* **43**, 1373-9.
- 433 **Korstanje, J. W., Scheltens-De Boer, M., Blok, J. H., Amadio, P. C., Hovius, S. E.,**
434 **Stam, H. J. and Selles, R. W.** (2012). Ultrasonographic assessment of longitudinal median
435 nerve and hand flexor tendon dynamics in carpal tunnel syndrome. *Muscle & Nerve* **45**, 721-9.
- 436 **Lance, V. A.** (2003). Alligator physiology and life history: the importance of
437 temperature. *Experimental Gerontology* **38**, 801-805.
- 438 **Lauder, G. V.** (1995). On the inference of function from structure. In *Functional*
439 *Morphology in Vertebrate Paleontology*, (ed. J. J. Thomason), pp. 1-18. New York: Cambridge
440 University Press.
- 441 **Lawson, A. B., Hedrick, B. P., Echols, S. and Schachner, E. R.** (2021). Anatomy,
442 variation, and asymmetry of the bronchial tree in the African grey parrot (*Psittacus erithacus*).
443 *Journal of Morphology* **282**, 701-719.
- 444 **Lessner, E. J., Dollman, K. N., Clark, J. M., Xu, X. and Holliday, C. M.** (2023).
445 Ecomorphological patterns in trigeminal canal branching among sauropsids reveal sensory shift
446 in suchians. *Journal of Anatomy* **242**, 927-952.
- 447 **Loram, I. D., Maganaris, C. N. and Lakie, M.** (2006). Use of ultrasound to make
448 noninvasive in vivo measurement of continuous changes in human muscle contractile length.
449 *Journal of Applied Physiology* **100**, 1311-1323.
- 450 **Mannion, P. D., Benson, R. B., Carrano, M. T., Tennant, J. P., Judd, J. and Butler,**
451 **R. J.** (2015). Climate constrains the evolutionary history and biodiversity of crocodylians.
452 *Nature Communications* **6**, 10.1038/ncomms9438.
- 453 **Molnar, J. L., Pierce, S. E., Bhullar, B. A., Turner, A. H. and Hutchinson, J. R.**
454 (2015). Morphological and functional changes in the vertebral column with increasing aquatic
455 adaptation in crocodylomorphs. *Royal Society Open Science* **2**, 10.1098/rsos.150439.
- 456 **Munns, S. L., Hartzler, L. K., Bennett, A. F. and Hicks, J. W.** (2005). Terrestrial
457 locomotion does not constrain venous return in the American alligator, Alligator
458 mississippiensis. *Journal of Experimental Biology* **208**, 3331-3339.

- 459 **Munns, S. L., Owerkowicz, T., Andrewartha, S. J. and Frappell, P. B.** (2012). The
460 accessory role of the diaphragmatic muscle in lung ventilation in the estuarine crocodile
461 *Crocodylus porosus*. *Journal of Experimental Biology* **215**, 845-852.
- 462 **Nesbitt, S. J.** (2011). The early evolution of Archosaurs: Relationships and the origin of
463 major clades. *Bulletin American Museum of Natural History* **352**, 1-292.
- 464 **Parrish, J. M.** (1986). Locomotor adaptations in the hindlimb and pelvis of the
465 Thecodontia. *Hunteria* **1**, 1-35.
- 466 **Parrish, J. M.** (1987). The origin of Crocodylian locomotion. *Paleobiology* **13**, 396-414.
- 467 **Perry, S. F.** (1988). Functional Morphology of the Lungs of the Nile Crocodile,
468 *Crocodylus niloticus*: Non-respiratory Parameters. *Journal of Experimental Biology* **134**, 99-117.
- 469 **Pizer, S., Amburn, E., Austin, J., Cromartie, R., Geselowitz, A., Greer, T., ter Haar**
470 **Romeny, B., Zimmerman, J. B. and Zuiderveld, K.** (1987). Adaptive histogram equalization
471 and its variations. *Computer Vision Graphics and Image Processing* **39**, 355-368.
- 472 **Salisbury, S. and Frey, E.** (2000). A biomechanical transformation model for the
473 evolution of semi-spheroidal articulations between adjoining vertebral bodies in crocodylians. In
474 *Crocodylian biology and evolution*, pp. 85-134. Chipping Norton: Surrey Beatty & Sons.
- 475 **Salisbury, S. W., Molnar, R. E., Frey, E. and Willis, P. M.** (2006). The origin of
476 modern crocodyliforms: new evidence from the Cretaceous of Australia. *Proceedings of the*
477 *Royal Society B: Biological Sciences* **273**, 2439-2448.
- 478 **Schachner, E. R., Lyson, T. R. and Dodson, P.** (2009). Evolution of the respiratory
479 system in nonavian theropods: evidence from rib and vertebral morphology. *Anatomical Record*
480 **292**, 10.1002/ar.20989.
- 481 **Schachner, E. R., Farmer, C. G., McDonald, A. T. and Dodson, P.** (2011). Evolution
482 of the dinosauriform respiratory apparatus: new evidence from the postcranial axial skeleton.
483 *Anatomical Record* **294**, 10.1002/ar.21439.
- 484 **Schachner, E. R., Diaz, R. E., Coke, R., Echols, S., Osborn, M. L. and Hedrick, B. P.**
485 (2022). Architecture of the bronchial tree in Cuvier's dwarf caiman (*Paleosuchus palpebrosus*).
486 *Anatomical Record*, 10.1002/ar.24919.
- 487 **Schachner, E. R., Lawson, A. B., Martinez, A., Grand Pre, C. A., Sabottke, C.,**
488 **Abou-Issa, F., Echols, S., Diaz, R. E., Jr., Moore, A. J., Grenier, J. P. et al.** (2023).
489 Perspectives on lung visualization: Three-dimensional anatomical modeling of computed and
490 micro-computed tomographic data in comparative evolutionary morphology and medicine with
491 applications for COVID-19. *Anat Rec (Hoboken)*.
- 492 **Schwab, J. A., Young, M. T., Neenan, J. M., Walsh, S. A., Witmer, L. M., Herrera,**
493 **Y., Allain, R., Brochu, C. A., Choiniere, J. N., Clark, J. M. et al.** (2020). Inner ear sensory
494 system changes as extinct crocodylomorphs transitioned from land to water. *Proc Natl Acad Sci*
495 *U S A* **117**, 10422-10428.
- 496 **Stockdale, M. T. and Benton, M. J.** (2021). Environmental drivers of body size
497 evolution in crocodile-line archosaurs. *Communications Biology* **4**, 38.
- 498 **Sullivan, C. S.** (2015). Evolution of hind limb posture in Triassic archosauriforms. In
499 *Great Transformations in Vertebrate Evolution*, eds. K. P. Dial N. H. Shubin and E. L.
500 Brainerd), pp. 107-124: University of Chicago Press.
- 501 **Thielicke, W. and Sonntag, R.** (2021). Particle Image Velocimetry for MATLAB:
502 Accuracy and enhanced algorithms in PIVlab. *Journal of Open Research Software* **9**,
503 10.5334/jors.334.

504 **Uriona, T. J. and Farmer, C. G.** (2006). Contribution of the diaphragmaticus muscle to
505 vital capacity in fasting and post-prandial American alligators (*Alligator mississippiensis*).
506 *Journal of Experimental Biology* **209**, 4313-4318.

507 **Uriona, T. J. and Farmer, C. G.** (2008). Recruitment of the diaphragmaticus,
508 ischiopubis and other respiratory muscles to control pitch and roll in the American alligator
509 (*Alligator mississippiensis*). *Journal of Experimental Biology* **211**, 1141-1147.

510 **Wang, T. and Warburton, S. J.** (1995). Breathing pattern and cost of ventilation in the
511 American alligator. *Respiration Physiology* **102**, 29-37.

512 **Wilberg, E. W.** (2015). What's in an outgroup? The impact of outgroup choice on the
513 phylogenetic position of Thalattosuchia (Crocodylomorpha) and the origin of Crocodyliformes.
514 *Systematic Biology* **64**, 621-37.

515 **Wilberg, E. W., Turner, A. H. and Brochu, C. A.** (2019). Evolutionary structure and
516 timing of major habitat shifts in Crocodylomorpha. *Science Reports* **9**, 514.

517 **Witmer, L. M.** (1995). The extant phylogenetic bracket and the importance of
518 reconstructing soft tissues in fossils. In *Functional morphology in vertebrate paleontology*, (ed.
519 J. J. Thomason), pp. 19-33. New York: Cambridge University Press.

520 **Young, M. T., Brusatte, S. L., Beatty, B. L., De Andrade, M. B. and Desojo, J. B.**
521 (2012a). Tooth-on-tooth interlocking occlusion suggests macrophagy in the mesozoic marine
522 crocodylomorph dakosaurus. *The Anatomical Record* **295**, 10.1002/ar.22491.

523 **Young, M. T., Brusatte, S. L., de Andrade, M. B., Desojo, J. B., Beatty, B. L., Steel,**
524 **L., Fernandez, M. S., Sakamoto, M., Ruiz-Omenaca, J. I. and Schoch, R. R.** (2012b). The
525 cranial osteology and feeding ecology of the metriorhynchid crocodylomorph genera Dakosaurus
526 and Plesiosuchus from the Late Jurassic of Europe. *PLoS ONE* **7**, 10.1371/journal.pone.0044985.

527

528

Figure 1

μ CT model and ultrasound positions.

(A) μ CT of *Alligator mississippiensis* (Hamilcar Barca) with a diagrammatic illustration of diaphragmaticus muscle (pink) and liver (gray) in left lateral view. White box represents the region enlarged in (B) which indicates the areas that ultrasound data were collected, represented from cranially to caudally: axillary (star), mid-thoracic (square), hepatic margin (hexagon), and post-hepatic (rectangle). (C) The ultrasound images are oriented in left lateral view with the most cranial region on the left edge of each image. The top of the video is the most superficial and the bottom the deepest. The brightest features in the videos are the ribs in white and the lung pleura running craniocaudal deep to the ribs. The pleura and ribs are visible in the axillary and mid-thoracic images. In the hepatic margin image, the liver is large, triangular in shape, and located in the center-right (caudal) region of the image. It is connected to the bright white lung pleura. In the post-hepatic image, the liver is in the far left (cranial) portion of the image and is connected to the diaphragmaticus muscle which runs craniocaudal. Deep to the diaphragmaticus muscle is the gastrointestinal system of the alligator.

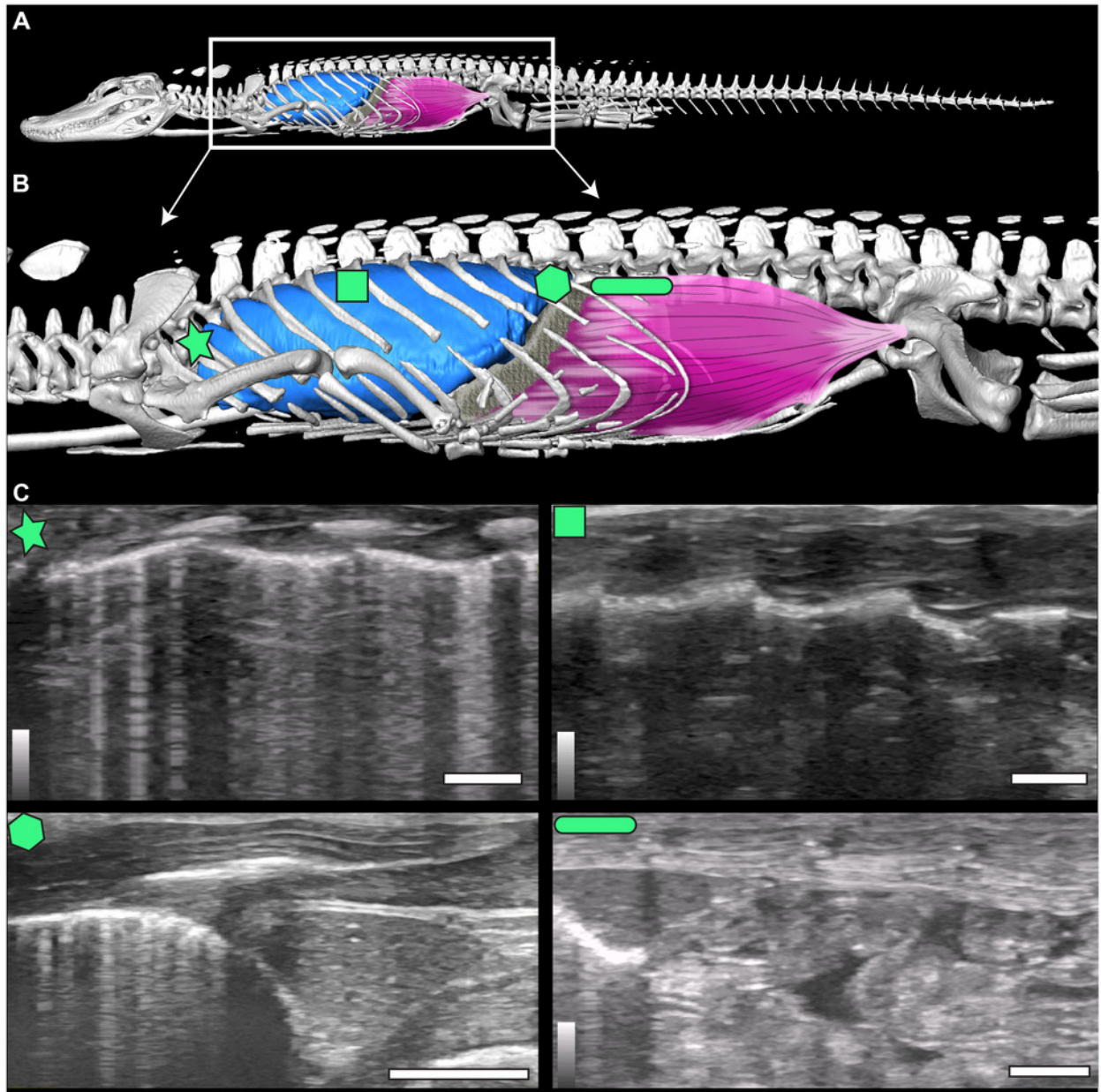


Figure 2

Osteological correlates constructed from segmented models of μ CT scans of *A. mississippiensis* (Hamilcar Barca).

On T1-T3 the parapophyses (pink circles with white lines) are located on the centra of the vertebrae and the diapophyses (blue circles with white outlines) are located on the transverse processes. Starting on T4 the parapophysis is located on the transverse process cranial to the diapophysis. This pattern continues to T11, the last thoracic vertebra. T3 is highlighted in mint green and exemplifies the forked rib morphology. T8 is in pink and exemplifies the smooth flat transverse process with smooth rib morphology. L3 in blue exemplifies the lumbar vertebrae. (A) Complete thoracic and lumbar vertebral column in left lateral view. (B) Complete thoracic and lumbar vertebral column in dorsal view. (C) Complete thoracic and lumbar vertebral column in ventral view demonstrating the smooth, flat thoracic ceiling—the result of the parapophyses joining the diapophyses on the transverse process. (D) T4, T8 and L3 in left lateral view. (E) T4, T8 and L3 in dorsal view. (F) T4, T8 and L3 in cranial view. (G) Rib 3 in cranial view highlighting the forked shape and Rib 8 in cranial view demonstrating the smooth flat shape.

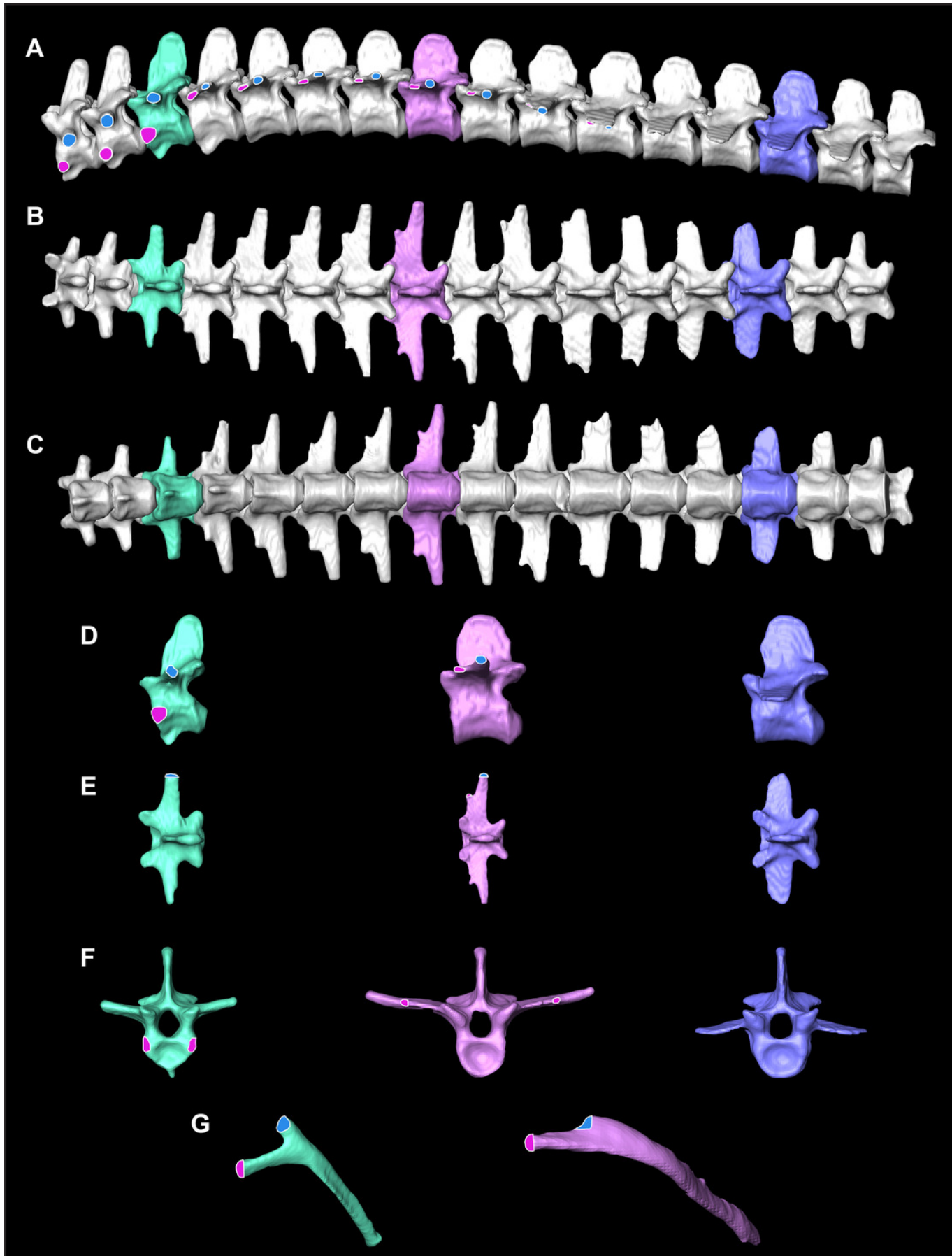


Figure 3

Thoracic ceiling of *A. mississippiensis*.

All viscera have been removed, demonstrating the smooth interior formed by the morphology of the axial skeleton. Cranial is to the left side of image. Scale bar = 2 cm.



Figure 4

Breath cycles in *A. mississippiensis* (James Bond) measured in PIVlab.

(A) PIVlab selection rectangle over the area of interest of the hepatic margin on the cranial edge of the liver in the caudalmost position. (B) PIVlab selection rectangle over the area of interest of the hepatic margin on the cranial edge of the liver in the cranialmost position. (C) The corresponding breath cycle as measured in PIVlab. The black arrows correspond to image A and B from left to right, respectively.

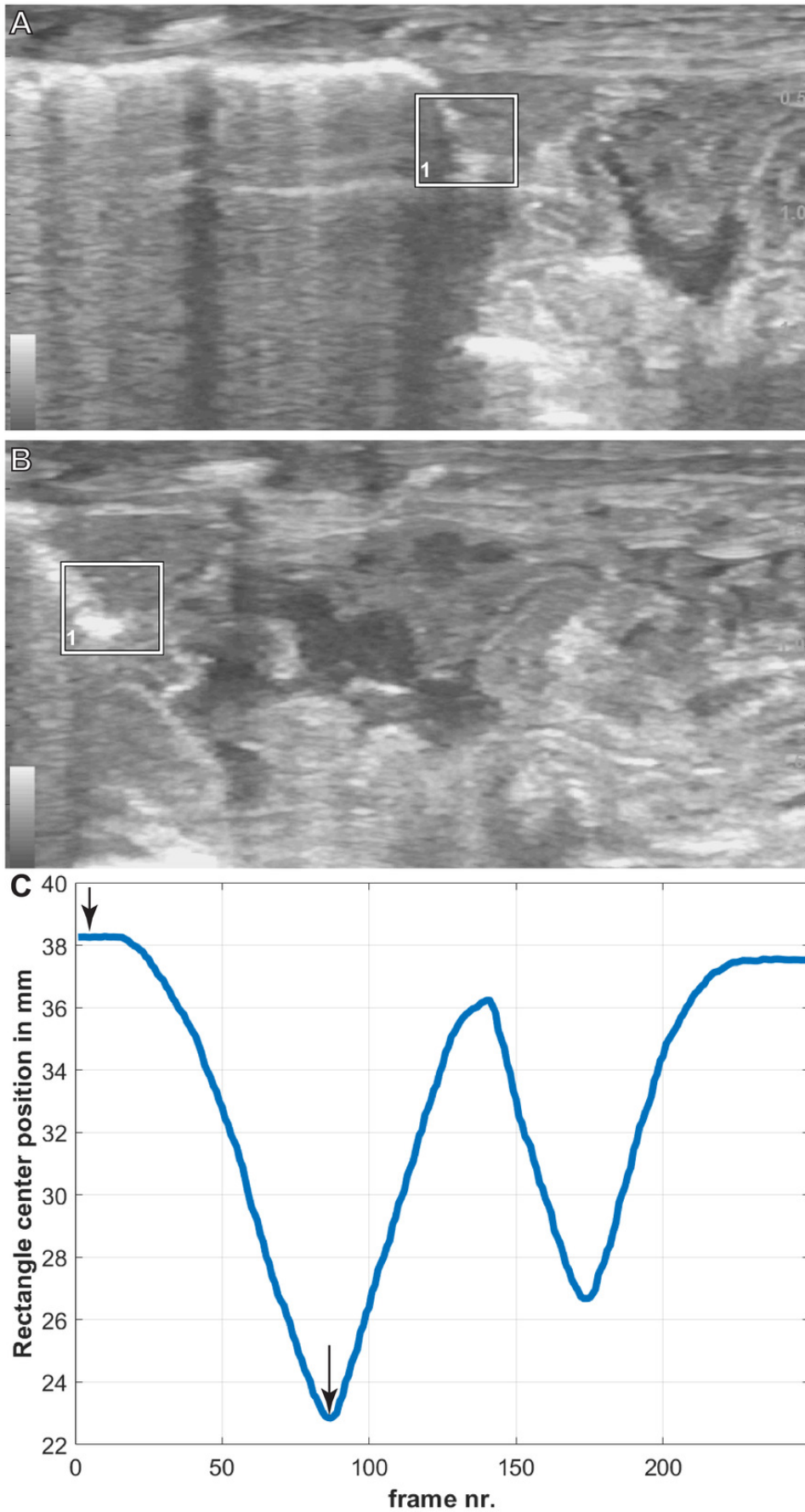


Figure 5

Statistical analyses of induced breaths and displacement related to size.

(A) Descriptive plot for James Bond (JB) and Marcus Claudius Marcellus (MC) illustrating the lack of a relationship between induced breaths (blue), breathing under normal atmospheric conditions (red), and displacement. (B) The trend is not significant between displacement (%) and SVL (cm). Each color represents a different specimen.

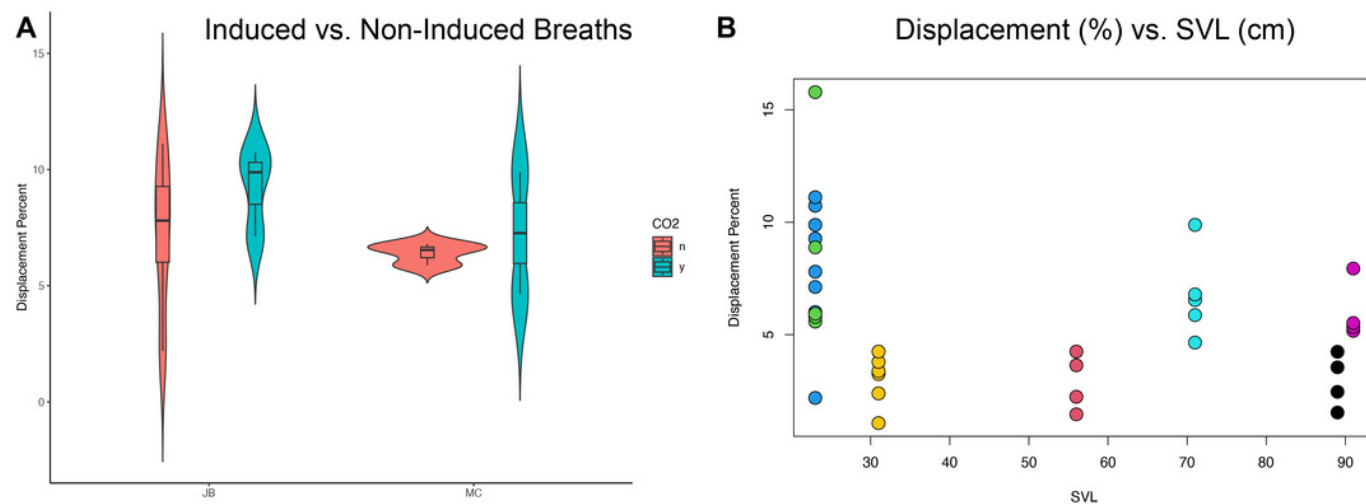


Table 1 (on next page)

Specimen data used in this study.

1

<i>Name of Specimen</i>	<i>Life Stage</i>	<i>SVL (cm)</i>	<i>Total Length (cm)</i>
Hannibal Barca	Juvenile	23	57
James Bond	Juvenile	23	58
Scipio Africanus	Juvenile	31	61
Gaius Claudius Nero	Sub-Adult	56	137
Marcus Claudius Marcellus	Sub-Adult	71	142
Archimedes of Syracuse	Adult	89	183
Quintus Fabius Maximus	Adult	91	185

2

Table 2 (on next page)

Manually acquired displacement measures at the hepatic margin as percent of SVL.

The *A. mississippiensis* specimens are listed in order of increasing SVL lengths. Values in grey boxes indicate ultrasound video was taken while the animal was breathing the 5% CO₂, balance N₂ gas.

1
2

Name	SVL (cm)	Displacement Percent (%)	Smallest Recorded Displacement (%)	Greatest Recorded Displacement (%)	Average Displacement (%)
Hannibal Barca	23	5.58 5.79 5.93 8.88 15.78	5.58	15.78	8.39
James Bond	23	2.19 6.01 7.12 7.80 9.27 9.88 10.73 11.11	2.19	11.11	8.01
Scipio Africanus	31	1.07 2.39 3.25 3.38 3.79 4.25	1.07	4.25	3.02
Gaius Claudius Nero	56	1.46 2.24 3.64 4.25	1.46	4.25	2.90
Marcus Claudius Marcellus	71	4.65 5.87 6.54 6.79 9.88	4.65	9.88	6.75
Archimedes of Syracuse	89	1.54 2.46 3.55 4.24	1.54	4.24	2.94
Quintus Fabius Maximus	91	5.17 5.34 5.52 7.94	5.17	7.94	5.99

3